Classification of wavelet decomposed AE signals based on parameter-less self organized mapping

G.Kalogiannakis*
Laboratory of Acoustics and Thermal Physics, Katholieke Universiteit Leuven, Belgium

D. Van Hemelrijck
Dept. Mechanics of Materials and Constructions, Vrije Universiteit Brussel, Belgium

*Georgios.Kalogiannakis@fys.kuleuven.be

Abstract - Composite materials are characterized by different types of failure mechanisms which are typically associated with matrix cracking, fiber-matrix debonding and fiber breakage. These three mechanisms result in a different AE signature, which can be often recognized. In certain cases it is necessary to classify and map the damage types so as to be able to evaluate the accumulated damage and remaining strength of the material. In this framework, neural networks are widely used for damage characterization. The classical approach involves recording waveform features and tries to associate them with the underlying damage source. Nevertheless, very often, it is very hard to draw definite conclusions based on these features. In this study, we have used a new type of a neural network which is called parameter-less self organized mapping. It is based on Kohonen neural networks but it is not bound to the naturally subjective learning rate, neighborhood function and their annealing with the training progress. Moreover, for the training of the NN and the subsequent classification, we have successfully used wavelet decomposed AE signals.

Keywords: acoustic emission, damage characterization, neural network, wavelet analysis.

1 Introduction

Acoustic emission (AE) can be ideally used to identify the underlying damage mechanisms of a structure under loading. The characteristics of the AE activity depend on the strain energy, which is released during a particular mechanism. The latter depends on the different stiffness, strength and toughness characteristics of the constituents (matrix, fibers and interphase between fibers and matrix), so that the different mechanisms are expected to generate distinct AE signals. The challenge is to be able to correlate the received signals with the corresponding mechanisms.

In this framework, there has been much work focused on training neural networks [1-2] in order to map the relationship between the AE features and the underlying damage mechanism and wavelet analysis [3-5] in order to investigate the correlation with both time and frequency information of the AE signals. For the former approach, in many cases it has been proven that it is generally hard to draw definite conclusions based on the AE features as they overlap for the different mechanisms depending on the loading phase.

In this work, we make use of a recent development of an initially unsupervised neural network (NN), called parameter-less self-organized mapping (PLSOM) to correlate and map partially integrated equidistant components of the wavelet coefficients of AE signals obtained from tensile tests of Glass/Polyester composites. The advantage of PLSOM is that it is not bound to the naturally subjective learning rate, neighborhood function and their annealing with the training progress. Moreover, the training of the NN with the wavelet decomposed AE signals allows for a more thorough investigation of the waveforms' frequency content as well as their evolution with time with respect to its generating source. A more detailed description of this work has been submitted for publication [6].

2 Material

The material tested was pultruded Glass/Polyester (supplied from Exel Composites nv). The selection was based on the particular application of this material for covering truck trailers, naturally susceptible to various mechanical wear mechanisms. Pultrusion is a manufacturing process for producing continuous lengths of reinforced plastic structural shapes with constant cross-sections. Rolls of fiberglass mat or doffs of fiberglass roving are saturated with a resin mixture ('wet-out' form) in the resin bath and then pulled through a heated die, curing and hardening the material profile according to its shape. The particular material we used for our experiments was in the form of symmetric thin plates consisting of five layers (Fig.1). The protective surface layers were relatively thin (0.1mm) with a special composition of polyester in the form of matrix reinforced with polyester fibers. The second layers were 0.8mm thick reinforced with fiberglass mat and the

intermediate layer was 1.6mm with unidirectional long fibers. The total fiber content in terms of volume fraction was 50 ± 5%.

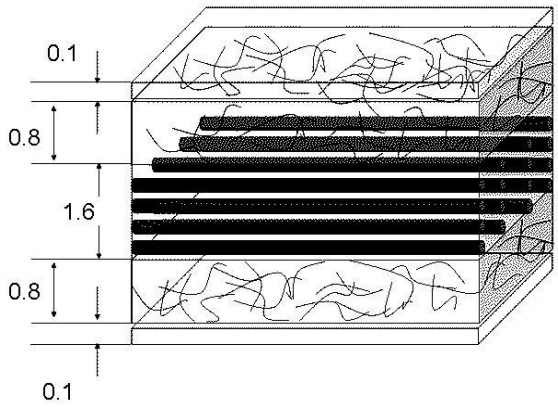

Figure 1. The stacking sequence of the tested composite material (the dimensions are given in mm).

3 Experimental procedure

The AE activity was monitored using DisP PCI-DSP4 of Physical Acoustics Corporation. The acquisition board allowed a maximum of 4 channels with simultaneous waveform recording at a maximum frequency of 10 MHz. After preliminary testing, peak definition, hit definition and hit lock-out values were set at 40, 300 and 500 μsec respectively. Waveforms were recorded with the aforementioned sampling rate for 600 μsec. The pre-amplifier gain was set at 40dB and the threshold for the signals' recording at 50dB due to the high sensitivity.

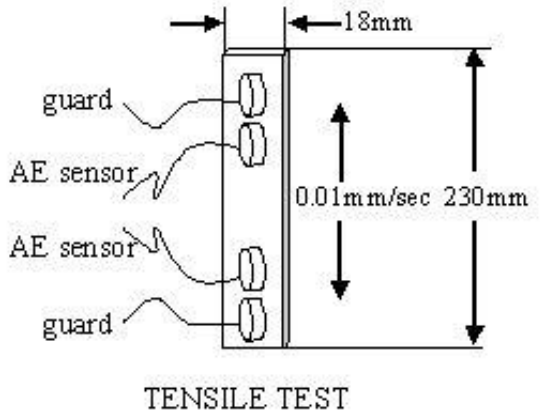

Figure 2: The experimental configuration used for tensile testing of pultruded Glass/Polyester rectangular thin specimens.

Tensile tests were conducted at room temperature with an INSTRON 4505 machine at a displacement rate of 0.01mm/sec. Four (4) AE broadband sensors (100-800kHz) were connected to the thin rectangular specimen (230mm x 18mm) used for this type of tests as shown in Figure 2. The two outer sensors were used as guards to prevent recording of signals originating from the grips. Experiments were performed with the fibers of the UD layer oriented both parallel and transverse to the direction of loading. Load and displacement were simultaneously recorded.

4 Wavelet decomposition of AE data

The wavelet transform (WT) is ideally used to analyze the frequency spectrum of signals [7], which are not stationary and such are the transient acoustic emission signals originating from growing damage in a material. The strength of WT is found in the capability of providing time and frequency information simultaneously giving a joint time-frequency representation of the signal which locates the appearance of particular spectral components in time. The continuous WT is defined as follows:

$$CWT_x^{\psi}(\tau,s) = \Psi_x^{\psi}(\tau,s) = \frac{1}{\sqrt{|s|}} \int x(t)\, \psi^*\left(\frac{t-\tau}{s}\right) dt \quad (1)$$

The signal in the wavelet domain is a function of τ and s, the translation and scale parameters respectively. The translation term is related to the location of the window (mother wavelet $\psi(t)$) as the window is shifted in time through the duration of the signal and the scale determines its size. As in the case of maps, high scale corresponds to non-detailed global view or low frequency and low scale corresponds to detailed view or high frequency.

For practical applications, the discrete wavelet transform (DWT) is more appreciated and widely used. The most common set of DWTs is the one formulated by Daubechies [8-9] and it is based upon the use of recurrence relations to generate progressively finer discrete samplings of an implicit mother wavelet function. The Daubechies wavelets are chosen to have the highest number of vanishing moments for a given support width. For the case under study 'Daubechies 14' or 'db14' was selected with the index number referring to the number of coefficients. The number of vanishing

moments for each wavelet is equal to half the number of coefficients, so 'db14' has 7 vanishing moments. A vanishing moment confines the ability of the wavelet to represent polynomial behaviour or otherwise information in a signal. For example, 'db2', with one vanishing moment, can easily represent polynomials of one coefficient or constant signals but it cannot encode in a satisfactory way higher order polynomials. On the other hand, increasing the number of coefficients has substantial influence on the computational requirements. Therefore, one has to find the most suitable wavelet that can represent the signal under investigation. In our case, 'db14' proved to be adequate for encoding the AE waveforms. Its scaling and wavelet functions of are shown in Figure 4.

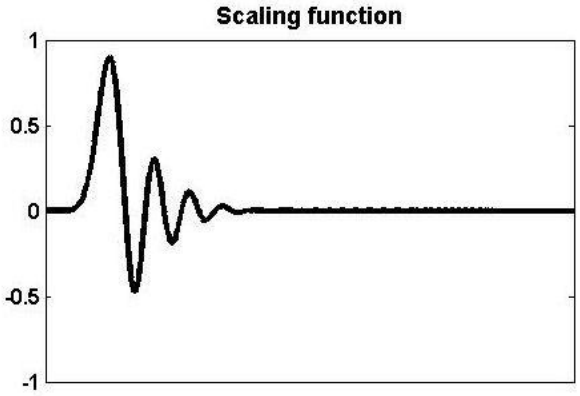

(a)

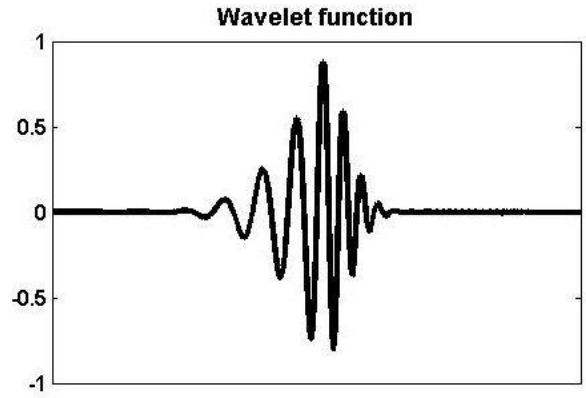

(b)

Figure 3. The scaling (a) and the wavelet (b) functions of Daubechies 14.

5 Parameter-less self-organized map

In the last part of this work, the wavelet decomposed AE data were classified using a known pattern recognition algorithm. A Kohonen Self-Organized Map (SOM) [10-11] was developed, which is an unsupervised neural network and can be used for the discrimination of classes or clusters (different types) in the AE signals. The map units or neurons are organized into a typically two-dimensional grid (Fig.4), with each neuron represented by a weight vector, which has the size of the input data. Such a neural network associates each of the input vectors containing AE signal features or elements associated with the wavelet decomposition with a particular output vector, a neuron, on the map, i.e. it organizes the input AE signals in such a way so that neighbors (similar AE signals) in the input data space are also neighbors in the grid.

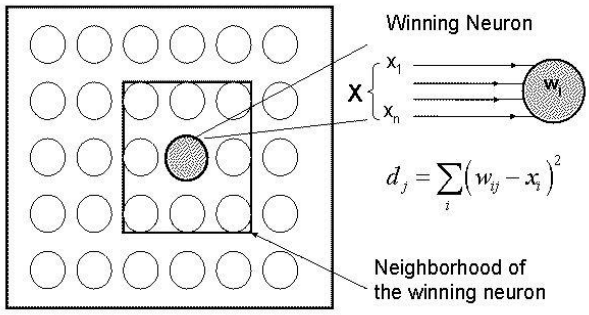

Figure 4. Self-organized map: the winning neuron for a specific input vector, is the one with the minimum Euclidean distance (the one most similar to the input). The winner and its neighborhood are updated to obtain the best fit for the input data.

The winning neuron for a specific input vector, is the one with the minimum Euclidean distance (the one most similar) as shown in Figure 3. In what follows, X is the input vector containing n components, w_i is the weight vector associated to neuron j with n components just like the input, m is the iteration count and d_j is the Euclidean distance of the input X to the neuron j. In the standard approach, the weights w_{ij} are adapted during a learning stage (training) based on the operation of the brain where similar signals stimulate contiguous neurons. After this stage, the map is organized in such a way that it represents topologically the different classes of input signals. As SOM is unsupervised, the number of classes needs no prior definition.

The iterative algorithm, which was used for the training of a SOM is the following:

1. Initialize all the weights to a random value between 0 and 1.

2. Select randomly an AE features vector and evaluate its Euclidean distance with respect to each neuron according to the equation:

$$d_j^m = \left\| \mathbf{X}^m - \mathbf{W}_j^m \right\|^2 = \sum_{i=1}^{n} \left(w_{ij}^m - x_i^m \right)^2 \quad (1)$$

3. Select the winning neuron k with minimum value of distance d_k

$$d_k^m = \min_{j \in 1 \ldots N} \left\| \mathbf{X}^m - \mathbf{W}_j^m \right\|^2 \quad (2)$$

where N is the total number of neurons on the map.

4. Update the weights of the winning neuron k as follows:

$$w_{ik}^{m+1} = w_{ik}^m + \eta^m \left[x_i^m - w_{ik}^m \right] \quad (3)$$

where m is the iteration count and η is a subjective gain representing how fast the neural network learns from the process and it is gradually reduced.

5. The neighbors of the winning neuron are also adapted. The size of the area, which describes the neighborhood, is defined according to a function *F(k)*. The latter determines how many neurons are updated close to the winning neuron. The size of the neighborhood is very significant for the learning process and it is also gradually reduced. However, in the standard approach, the selection of the neighborhood doesn't obey any particular rule leading to a rather subjective mapping.

$$w_{ij}^{m+1} = w_{ij}^m + \eta^m \left[x_i^m - w_{ij}^m \right], \; j \in F\ k \quad (4)$$

6. Repeat steps (1) to (5).

One of the major drawbacks of using self-organized maps (SOM) to visualize clusters of multidimensional data is their dependence on the learning rate, the size of the neighborhood as well as their annealing (process of decreasing) with the training [12]. The first parameter is decisive with respect to the convergence speed of the neural network. The updated values of the weights depend on their error with respect to the input, but to achieve a stable convergent state we must define a learning rate. This learning rate is large at the beginning when the map is unordered and fits the input space poorly and it decays as the training progresses. The problem is that there is no firm theoretical way to estimate this learning rate. This led to the search of a method by which the optimal learning rate and decay can be determined with mathematical certainty. One of the latest methods [12], the so-called PLSOM, lets the scaling of the weight vector update function as well as the size of the neighborhood depend on internal conditions in the SOM. The internal condition for scaling these variables is the least error ε^m, i.e. the normalized Euclidean distance from the input to the closest weight vector after the iteration count m.

$$\varepsilon^m = \frac{\left\| \mathbf{X}^m - \mathbf{W}_k^m \right\|^2}{\rho^m} \quad (5)$$

where

$$\rho^m = \max \left\| X^m - W_k^m \right\|^2, \rho^{m-1} \;,$$
$$\rho^0 = \left\| X^0 - W_k^0 \right\|^2 \quad (6)$$

According to PLSOM, it is intuitive that if ε^m is large, the map needs to change more to accommodate future inputs of this class, but if it is small the fit is already good and there is no need for large alterations of the map. So, PLSOM relies on the idea that the learning rate and the neighborhood size should not vary according to the iteration number but rather according to whether the map represents well the topology of the map.
The size of the neighborhood is also a function of ε^m and it is determined as follows:

$$\Theta^m = \beta^m \varepsilon^m \quad (7)$$

where β^m is the previously variable size of neighborhood, which is now constant. So, *F(k)* is a scaling function centered on the winning neuron k decreasing (we consider an exponential decay) in all directions, which can be expressed as:

$$F^m\ k = \exp\left[-\left(\frac{d^m\ j,k}{\Theta^m} \right)^2 \right] \quad (8)$$

where $d^m(j,k)$ is the Euclidean distance from the neuron j to the winning neuron k.

The expression for the weight update of the winning neuron and its neighborhood can be formulated as:

$$w_{ij}^{m+1} = w_{ij}^m + \varepsilon^m F^m\ k \left[x_i^m - w_{ij}^m \right] \quad (9)$$

6 Results – Discussion

Tensile tests were conducted with specimens having the fibers of the UD layer positioned parallel (2 tests) as well as transverse (2 tests) to the direction of loading. Tensile testing is ideally suitable for the correlation of each damage type with the generation of a particular AE waveform as damage evolution and characterization are well described in the literature and can be used as guides for our study. In short, for both types of specimens, damage initiates with matrix micro-cracking due to its lower toughness. Matrix micro-cracks gradually evolve, propagate and coalesce to form macro-cracks, which reach the borders with the fibers. The stress concentration around those points becomes so large that it eventually exceeds either the strength of the bond between the matrix and the fiber or the strength of the fiber itself. As a result, for the first case, the crack propagates along the interphase between the fiber and the matrix, debonding thus the fiber, which is gradually pulled out. In the second case, the reinforcing strong and brittle glass fiber breaks instantaneously, releasing a relatively large amount of energy.

Each of the damage types generate an AE signal, which is closely related to the amount of strain energy that is released as well as the ductile or brittle type of fracture. Therefore the corresponding signal waveform has features, like e.g. energy or duration as well as frequency content, which are representative for the type of the underlying failure. The reason that we performed experiments for the two previously given different types of specimens is that the main mechanism, which leads to global failure, is different [6].

For the specimens with the fibers of the UD layer parallel to the loading direction, global failure arrives with extended fiber breakage and delaminations between the mat and the UD layer. The first effect originates from the strong normal stresses, which develop on the fibers and the latter effect originates from strong interlaminar shear stresses at the interface between the mat and the UD layer. On the other hand, for the second type of specimens with the fibers in the transverse direction, global failure is highly localized around the central portion of the long specimens and driven by extended debonding of the fibers. It is evident that this debonding originates from a combination of strong normal and shear stresses, which develop at the interphase.

These facts can help us a lot in the distinction of the different AE signals and their correlation with each of the particular damage types. The association of the signals received with the relevant damage is carried out by studying firstly their timely occurrence for both specimens and secondly by comparing their relative number with respect to the type of specimen. In what follows in this section, we will be based on the association made in [6], where thorough investigation showed that: (a) fiber breakage generates mid to high amplitudes at short durations with high frequency content, (b) matrix cracking has low to mid amplitudes, short durations and mid frequency content and finally (c) fiber debonding as well as delaminations generate AE hits which cover the whole range of amplitudes and typically have long durations and low frequency content.

In this framework, we have studied the possibility to classify and map these AE signals based on their wavelet transforms. It should be stressed that no special analysis was performed to involve the attenuation and change of the AE signals with distance as preliminary evaluation showed that the sensors were adequately close to one another as well as the center of the sample to disregard the attenuation.

The procedure which was followed for the classification can be summarized as follows:

- Recording of AE waveforms.
- Normalization with respect to max amplitude.
- Wavelet decomposition to the maximum level.
- Normalization of the derived coefficients.
- (Partial) Integration for each scale in 6 equidistant time windows.
- Creation of the wavelet input vectors having 30 (5 scales x 6 windows) components.

In order to map the different classes with the PLSOM, we had to select a certain number of data for the training of the neural network. In order to facilitate the classification a method was used that renders the neural network supervised [1]. 9 representative groups of 50 wavelet decomposed data vectors were selected by finding the 9 most distant input vectors and using them as guide to find the 50 closest vectors to each one of them. To determine them, all distances between data pairs were calculated and the highest valued pair was selected and added to an initially empty set of most distant input items. Then the 50 closest vectors to the ones selected were added to their group and removed from the input data. Afterwards the next most distant input to the ones already selected were added to the set and so on. The 9 most representative vectors were also used to initialize the self-organized map as potential cluster centers. This technique prevents us from variable classification performance and time consuming training iterations on the same data. It should be clarified that the number of clusters that will be used is not a very significant prediction in absolute terms. It just has to be large enough to fit the classification and if it is too large, the PLSOM will appear to have unifying clusters.

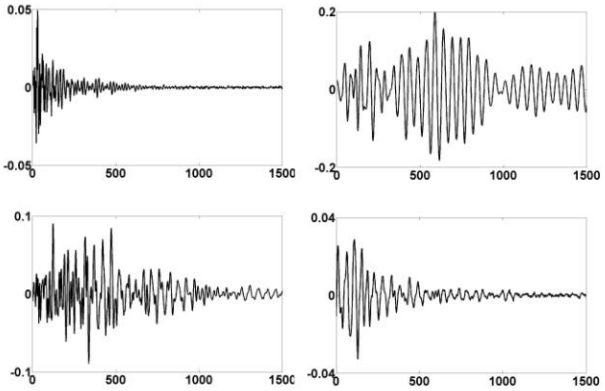

Figure 5. Typical waveforms which represent the centers of 4 different clusters.

Figure 5 shows some typical waveforms which represent the different damage mechanisms or, in classification terms, the centers of 4 different clusters. These were found based on the Euclidean distances of the wavelet decomposed signals which are shown in Figure 6 before integration. The level of decomposition is associated to the frequency and the x-axis relates to time. The pseudo-frequencies corresponding to the decomposition levels are f= [1724 862 431 215 107] kHz. To carry out the selection, the wavelet decomposed AE data were reshaped in one-dimensional vectors which were then integrated as shown in Figure 7.

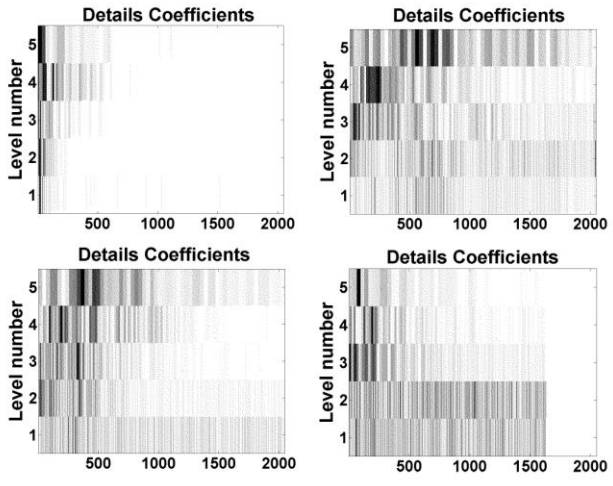

Figure 6. The corresponding wavelet transforms of the waveforms depicted in Figure 5.

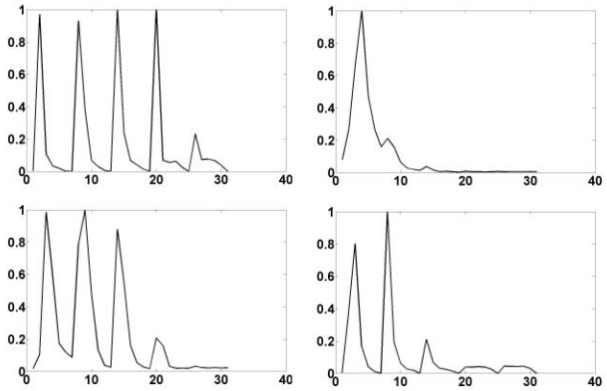

Figure 7. Partially integrated wavelet decomposed input vectors for the 4 different classes depicted in Figures 5 and 6.

It is clear in all three figures (waveform representation, wavelet decomposed signals and partially integrated vectors) that there is a clear distinction based on the underlying mechanism that relates to the waveform frequency content and its evolution as well as the duration. It is also evident that the average frequency content is not adequate to characterize the mechanism as there is often an alteration with time.

Afterwards, the input vectors were classified by means of a 48x48 PLSOM as shown in Figure 8. The image visualizes the Euclidean distance of neighboring elements and the different classes are clearly distinct. Dark areas designate the borders of clusters with darker colors indicating larger distance or bigger difference between neighboring clusters. This map was trained with 50 epochs and can serve for the classification of any incoming AE signal of similar conditions tensile testing.

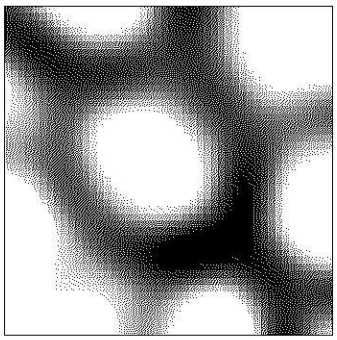

Figure 8. The PLSOM trained with partially integrated wavelet decomposed vectors as shown in Figure 7.

7 Conclusions

An unsupervised neural network was successfully used to classify AE data based on their partially integrated wavelet transforms; an approach that appears to be a significant improvement with respect to the efficiency of conventional techniques.

References

[1] T.P.Philippidis, V.N.Nikolaidis, A.A.Anastassopoulos Damage characterization of carbon/carbon laminates using neural network techniques on AE signals. NDT&E International 31(5):329-340, 1998.
[2] G.Kalogiannakis, J.Quintelier, P.De Baets, J.Degrieck, D.Van Hemelrijck. Identification of wear mechanisms of Glass/Polyester composites by means of acoustic emission. Wear (in press)
[3] G.Qi. Wavelet-based characterization of composite materials. NDT&E International 33 : 133-144, 2000.
[4] Qing-Qing Ni & M.Iwamoto. Wavelet transform of acoustic emission signals in failure of models composites. Engineering Fracture Mechanics 69: 717-728, 2002.
[5] M.Johnson. Classification of AE transients based on numerical simulations of composites laminates. NDT&E International 36 : 319-329, 2003.
[6] G.Kalogiannakis, J.Quintelier, P.De Baets, J.Degrieck, D.Van Hemelrijck. Damage characterization of pultruded Glass/Polyester based on wavelet and cluster analysis of AE data. Submitted in *Composites Science and Technology*
[7] R.K.Young, *Wavelet theory and its applications*. Boston: Kluwer Academic, 1994.
[8] I.Daubechies. Orthonormal bases of compactly supported wavelets. Communications on pure and applied mathematics 41(7): 909-996, 1988.
[9] I.Daubechies. The wavelet transform, time-frequency localization and signal analysis. *IEEE transactions of information theory* 36(5): 961-1005, 1990.
[10] T.Kohonen. *Self-organisation and associative memory*. Berlin: Springer, 1988.
[11] T.Kohonen. Self-organised network. In Proc. IEEE 43:59-69, 1990.
[12] E.Berglund and J.Sitte. The Parameter-Less SOM algorithm. In Proc. of 8th Australian and New Zealand Intelligent Information System Conference (ANZIIS '03), Sydney, Australia, 2003.